Redox Control of the Catalytic Cycle of Flavocytochrome P-450 BM3[†]

S. N. Daff, S. K. Chapman, K. L.Turner, R. A. Holt,[‡] S. Govindaraj,[§] T. L. Poulos,[§] and A. W. Munro*

Department of Chemistry, University of Edinburgh, The King's Buildings, West Mains Road, Edinburgh, EH9 3JJ U.K., Zeneca Life Science Molecules, Biomolecules, P.O. Box 2, Belasis Avenue, Billingham, Cleveland, TS23 1YN U.K., and Departments of Molecular Biology and Biochemistry, and Physiology and Biophysics, University of California, Irvine, California 92697-3900

Received May 8, 1997; Revised Manuscript Received August 7, 1997[⊗]

ABSTRACT: Flavocytochrome P-450 BM3 from *Bacillus megaterium* is a 119 kDa polypeptide whose heme and diflavin domains are fused to produce a catalytically self-sufficient fatty acid monooxygenase. Redox potentiometry studies have been performed with intact flavocytochrome P-450 BM3 and with its component heme, diflavin, FAD, and FMN domains. Results indicate that elctron flow occurs from the NADPH donor through FAD, then FMN and on to the heme center where fatty acid substrate is bound and monooxygenation occurs. Prevention of futile cycling of electrons is avoided through an increase in redox potential of more than 100 mV caused by binding of fatty acids to the active site of P-450. Redox potentials are little altered for the component domains with respect to their values in the larger constructs, providing further evidence for the discrete domain organization of this flavocytochrome. The reduction potentials of the 4-electron reduced diflavin domain and 2-electron reduced FAD domain are considerably lower than those for the blue FAD semiquinone species observed during reductive titrations of these enzymes and that of the physiological electron donor (NADPH), indicating that the FAD hydroquinone is thermodynamically unfavorable and does not accumulate under turnover conditions. In contrast, the FMN hydroquinone is thermodynamically more favorable than the semiquinone.

The cytochromes P-450 are a diverse group of hemoproteins which catalyze a plethora of oxidative reactions in organisms from all known Phyla. Indeed, the discovery of a P-450 in a member of the archae indicates that the P-450s occurred very early in evolution (Wright *et al*., 1996). The vast majority of these reactions result from the insertion of a single atom of molecular oxygen into organic substrates, with the other atom converted into water. Electron equivalents are supplied by NAD(P)H via different redox partners. Class I (or B) type P-450s are usually reduced by an iron sulfur protein (ferredoxin), which receives electrons from an FAD-containing ferredoxin reductase. These systems are typified by bacterial forms (hence B-type), the most intensively studied form being the camphor hydroxylase (P-450cam) from *Pseudomonas putida* (Poulos *et al.*, 1987). Class II (or E-type) P-450s are reduced by a diflavin (FAD- and FMN-containing) NADPH-cytochrome P-450 reductase (Munro & Lindsay, 1996). These systems are typified by the liver microsomal enzymes involved in mammalian drug/steroid metabolism. Certain mammalian members of this class are also implicated in activation of carcinogens (Guengerich, 1988). Obvious advantages exist for the application of specroscopic studies to the bacterial P-450s over the eukaryotic class II forms. Firstly, the problems of protein purification and gene isolation/overexpression are simplified for the soluble prokaryotic forms. In addition, problems exist with the maintenance of the membranous forms in suspension at sufficiently high concentration.

The identification of a soluble bacterial class II P-450 by the group of Armand Fulco at UCLA (Narhi & Fulco, 1986) has provided an attractive model system for the mammalian systems. P-450 BM3 from *Bacillus megaterium* is expressed naturally at high levels and is a fusion protein, comprised of the components of the class II system joined in a continuous polypeptide by a short hydrophilic linker chain (Munro *et al.*, 1994). The gene encoding P-450 BM3 (*cyp*102) has been cloned and overexpressed in *Escherichia coli*, as have the genes encoding its component heme and diflavin domains (Narhi & Fulco, 1987; Miles *et al*., 1992), facilitating the production of protein in large quantities for studies with a variety of biophysical techniques.

Electron flow to the heme iron in P-450cam is known to be controlled by a camphor-dependent increase in the redox potential of the heme iron, previously measured as −303 mV (substrate free) to −173 mV (camphor bound) (Sligar & Gunsalus, 1976) and more recently as −330 mV to −163 mV (Martinis *et al.*, 1996). Removal of water molecules from the environment of the heme (most notably the water which provides the sixth ligand to the iron in the resting state) accompanies binding of camphor and the resultant change in spin-state and local dielectric constant underlies the large increase in reduction potential seen. The camphor-bound potential is higher than that of the redox partner (putidaredoxin at −240 mV), and electron transfer to the heme can occur. This elegant control system prevents futile cycling of electrons. Binding of dioxygen follows single electron reduction of the heme iron and leads to the formation of the ferrous−dioxygen intermediate [best described as superoxide attached to ferric iron (Mueller *et al.*, 1995)].

[†] The authors wish to thank the Royal Society of Edinburgh for the awards of a Caledonian Foundation Research Fellowship (A.W.M.) and an SOEID Fellowship (S.K.C.). We also wish to thank the BBSRC for their support of these studies (studentships to S.N.D. and K.L.T.)

* Author to whom correspondence should be addressed. Tel: +44 131 650 4753. Fax: +44 131 650 4760. E-mail: Andrew.Munro@ed.ac.uk.

[‡] Zeneca Life Science Molecules.

[§] University of California.

[⊗] Abstract published in *Advance ACS Abstracts,* October 1, 1997.

[1] Abbreviations: IPTG, isopropyl-β,D-thiogalactopyranoside; O.D., optical density; P-450, cytochrome P-450 monooxygenase; PMSF, phenylmethanesulfonyl fluoride.

S0006-2960(97)01085-4 CCC: $14.00

This high-potential species is further reduced rapidly by a second electron to form the unstable high valency ferryl iron-oxygen center which is responsible for the cleavage of the dioxygen bond. A single atom of oxygen is inserted into the substrate, with the other atom reduced to water.

P-450 BM3 provides an elegant system for the analysis of redox control of catalysis in a class II P-450 system. In this manuscript, we present potentiometric data collected for intact P-450 BM3 and for each of its component domains (heme [P-450], diflavin [reductase], FAD and FMN). Studies on the isolated domains (particularly the flavin-containing domains) are vital for the deconvolution of complex visible spectroscopic changes, which for the holoenzyme, may result from contributions from three different chromophores. The analysis of the effect of substrate binding to the heme domain on the reduction potential of this center is important for the understanding of the means by which electron transfer from the flavins is controlled. Data presented here permit the construction of a pathway for electron flow through the entire flavocytochrome enzyme.

EXPERIMENTAL PROCEDURES

E. coli Strains and Plasmid Vectors. *E. coli* strain TG1 [*sup*E, *hsd*Δ5, *thi*, Δ(*lac-pro*AB), F′ [*tra*D36, *pro*AB$^+$, *lac*I^q, *lac*ZΔM15]] was used for all cloning work and for overexpression of intact P-450 BM3 and its component diflavin and heme domains. Strain BL21 (DE3) (*hsd*S, *gal*, [λ*c*I*ts*857, *ind*1, Sam7, *nin*5, *lac*UV5-T7 gene 1]) was used for overexpression of the FAD- and FMN-containing domains of P-450 BM3. The preparation of constructs for the overexpression of intact P-450 BM3 (construct pBM25) and of its component diflavin (reductase, initiating methionine and residues 473 to the end; construct pBM27) and heme (P-450, residues 1−472; construct pBM20) domains has been presented in previous publications (Miles *et al.*, 1992, Munro *et al*., 1996). The preparation of constructs encoding the FAD (residues 654−1048) and FMN (471−664) domains has also been outlined in a recent publication (Govindaraj & Poulos, 1997). In all cases, expression is from inducible promoters (*lac* for intact P-450 BM3 and heme domain, *tac* for diflavin domain, and T7 for FAD and FMN domains).

Enzyme Preparations. Intact cytochrome P-450 BM3 and its component heme and diflavin domains were purified as outlined previously (Miles *et al.*, 1992). IPTG addition (500 μg/mL final concentration) was made to cultures grown at 37 °C in Terrific Broth at an O.D. at 600 nm of approximately 1.0. Thereafter, the temperature was decreased to 30 °C and culture was continued for another period of 12 h. A final gel filtration step (Sephacryl S-300HR) was used to remove minor contaminating protein species. PMSF (1 mM) and leupeptin (1 mM) were added to all buffers to minimize proteolysis. Overexpression of the FAD and FMN domains was carried out as described previously (Govindaraj & Poulos, 1997). The FAD domain was purified in identical fashion to intact P-450 BM3 (ion exchange chromatography on DEAE-Sephacel followed by affinity chromatography on 2′5′-ADP sepharose), with the exception that an initial 0−60% ammonium sulfate pellet of the *E. coli* transformant extract was used as a starting point for the purification (rather than a 30−60% pellet for intact P-450 BM3). The FMN domain was prepared essentially as described previously (Govindaraj & Poulos, 1997), again using a 0−60% ammonium sulfate pellet as the starting point for the purification and performing successive steps of ion exchange chromotography (DEAE Sephacel; loaded in buffer A (50 mM Tris·HCl, pH 7.3) and eluted with a linear gradient of 0 to 500 mM KCl in the same buffer) and gel filtration (Sephacryl S-100HR, column size approx. 2 cm × 1.5 m, buffer A). All proteins were stored at −20 °C after dialysis into a 500× volume of buffer A containing 50% glycerol and protease inhibitors, and used within 1 month of manufacture.

Potentiometric Titrations. All redox titrations were conducted within a Belle Technology glovebox under a nitrogen atmosphere, with oxygen maintained at less than 5 ppm. Degassed, concentrated enzyme samples were passed through an anaerobic Sephadex G25 column (1 × 20 cm) (Sigma) immediately on admission to the glovebox, thereby removing all traces of oxygen. The column was equilibrated and enzyme eluted with 0.1 M phosphate buffer, pH 7.0, which was used throughout this experimental procedure. Enzyme solutions were titrated electrochemically according to the method of Dutton (1978) using sodium dithionite as reductant and potassium ferricyanide as oxidant. Mediators were introduced prior to titration, typically 5 μM 2-hydroxy-1,4-napthaquinone, 1 μM benzyl viologen, and 1 μM methyl viologen (Sigma) within sample volumes of 3−10 mL. After 10−15 min equilibration following each reductive/oxidative addition, spectra were recorded on a Shimadzu 2101 UV−vis spectrophotometer (typically between 350 and 800 nm) contained within the anaerobic environment. The electrochemical potential of the sample solutions were monitored using a CD740 meter (WPA) coupled to either Pt/calomel or Pt/Ag·AgCl combination electrodes (Russell pH Ltd.) at 25 ± 2 °C. The electrodes were calibrated using the Fe^{III}/Fe^{II} EDTA couple as a standard (+108 mV). The calomel and Ag·AgCl electrodes were corrected by +244 ± 2 mV and +198 ± 3 mV respectively, both relative to the normal hydrogen electrode. For experiments involving the flavin-containing domains, UV−vis spectra were affected by an increase in baseline with time due the slow formation of a protein precipitate. Data collected for the FAD domain was affected most significantly. This was corrected for by transforming each spectrum with a $1/\lambda$ subtraction calculated to return the absorbance at 800 nm back to zero (at this wavelength chromophore absorbance is minimal). The same procedure was used to correct data collected for the FMN and diflavin domains. All data manipulations and nonlinear least-squares curve fitting of electrochemistry data was conducted using Origin (Microcal).

For redox titrations of the heme domain in the presence of substrate, the substrate was titrated into the enzyme solution while the change in spin state was monitored spectrophotometrically. The substrates used were laurate, myristate, palmitate, and arachidonate (all from Sigma), added in microliter amounts from concentrated solutions in 50/50 (v/v) methanol/ethanol. The K_m values for these substrates are approximately 100, 15, 2, and 2 μM, respectively. Substrate was added until no further change in the visible spectrum occurred (approx. 1 mM, 400, 300, and 300 μM, respectively). Redox titrations of substrate/enzyme mixtures were conducted as described above.

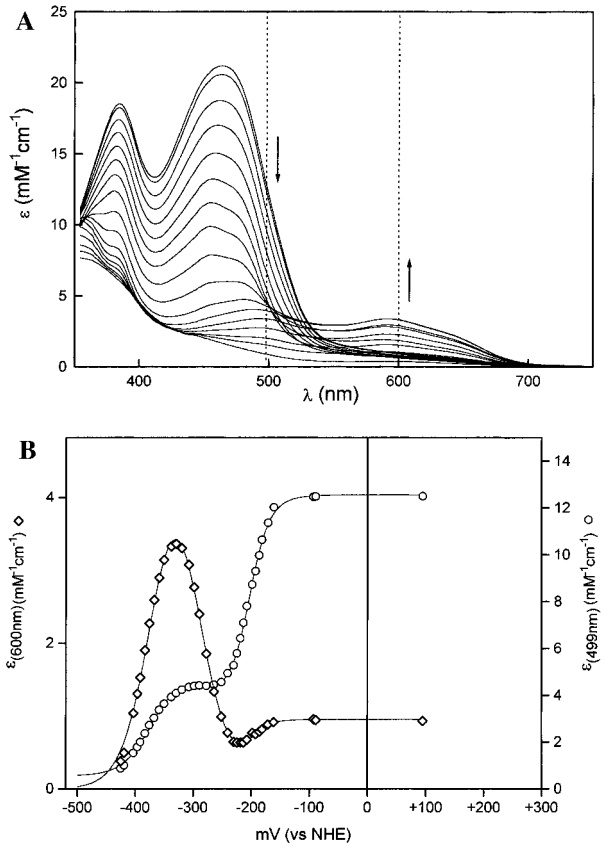

FIGURE 1: (A) Redox titration of P-450 BM3 diflavin domain conducted in 0.1 M phosphate buffer (pH 7.0) at 25 ± 2 °C. Directions of arrows indicate absorbance decreases at 499 nm and increases at 600 nm during the course of the reductive titration. (B) Plot of extinction coefficient versus electrode potential at 499 nm (right *y*-axis) and 600 nm (left *y*-axis) fitted to eq 1 as described in the Results. From the 499 nm data, E_1' (FMN) = −213 ± 5 mV and E_2' (FMN) = −193 ± 6 mV; from the 600 nm data, E_1' (FAD) = −292 ± 4 mV and E_2' (FAD) = −372 ± 4 mV.

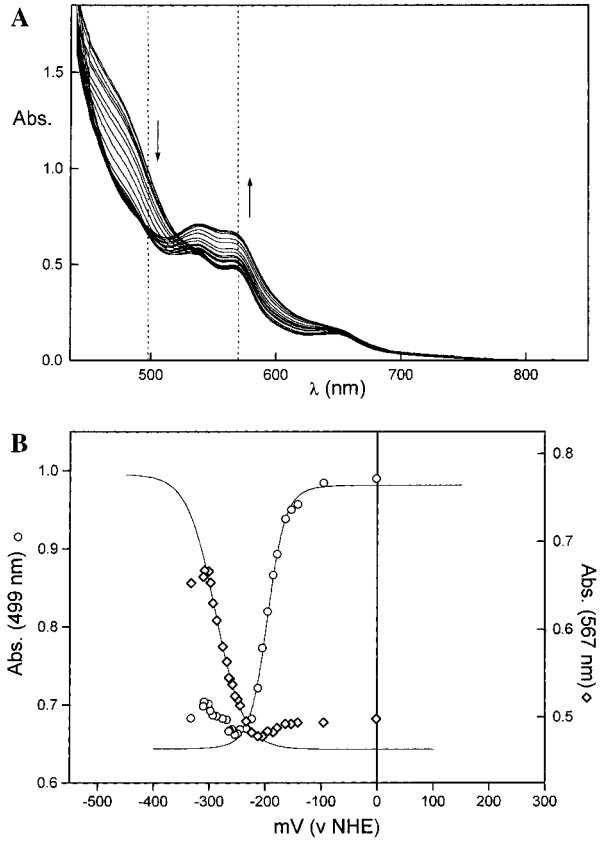

FIGURE 2: (A) Redox titration of P-450 BM3 holoenzyme conducted in 0.1 M phosphate buffer (pH 7.0) at 25 ± 2 °C. Directions of arrows indicate absorbance decreases at 499 nm and increases at 567 nm during the course of the reductive titration. (B) Plot of absorbance versus electrode potential at 499 nm (left *y*-axis) and 567 nm (right *y*-axis) fitted to two-electron and one-electron functions, respectively, as described in the Results. From the 499 nm, data E_1' (FMN) = −216 ± 11 mV and E_2' (FMN) = −177 ± 11 mV; from the 567 nm data E_1' (FAD) = −289 ± 4 mV.

RESULTS

Potentiometric Titrations. Diflavin Domain. Figure 1A shows the redox titration of the P-450 BM3 diflavin domain monitored by UV−vis spectrophotometry between 350 and 800 nm. Figure 1B plots the values for absorbance at 499 and 600 nm against the potential of the enzyme solution. Although not strictly an isosbestic point for the FAD oxidized/semiqinone couple, inspection of Figure 3A revealed that 499 nm was the wavelength at which minimum absorbance change occurred over the −100 to −300 mV range in which the FMN redox change occurs. Similarly, a convenient wavelength at which to monitor the FAD redox change [from inspection of Figure 3 (panels A and b)] is 600 nm. The absorbance *vs* potential data is fitted in Figure 1B to an equation (eq 1) comprising the sum of two two-electron redox functions designed to model the absorbance of a flavin passing through three different oxidation states. The parameters E_1' and E_2' were only allowed to vary in one of the two functions at any one time such that the values derived from the data at 499 nm were fixed during the fitting of the data at 600 nm and *vice versa*. Fitting was completed when further iterations of this procedure produced no change. In this way, values for the FMN reduction potentials were derived from the data collected at 499 nm, while values for the FAD reduction potentials were derived from the data collected at 600 nm:

$$\text{Flavin absorbance} = \frac{a10^{(E-E_1')/59} + b + c10^{(E_2'-E)/59}}{1 + 10^{(E-E_1')/59} + 10^{(E_2'-E)/59}} \quad (1)$$

where *a*, *b*, and *c* are the absorbance coefficients for oxidized, semiquinone, and reduced flavin, respectively, *E* is the electrode potential, and E_1', and E_2' are the midpoint potentials for the oxidized/semiquinone couple and the semiquinone/reduced couple, respectively.

Values for the redox potentials of the FMN and FAD of the diflavin domain are collated in Table 1. While the potentials for the two one-electron couples of the FAD are well separated, this is not the case for the FMN. Here, the first couple (E_1') is more negative than the second (E_2') by only 20 mV. Thus, the two processes appear to happen simultaneously and the data can be represented reasonably well by a two-electron function. As a result, the midpoint potentials derived for the individual steps may underestimate slightly the magnitude of the separation, although the value for the two-electron process remains accurate.

Holoenzyme. Figure 2A shows the redox titration of the P-450 BM3 holoenzyme between 450 and 850 nm. Figure 2B plots values for absorbance at 499 and 567 nm against the electrode potential. As explained in the previous section, 499 nm is a convenient wavelength at which to observe FMN reduction. Since the reduction potential of the heme

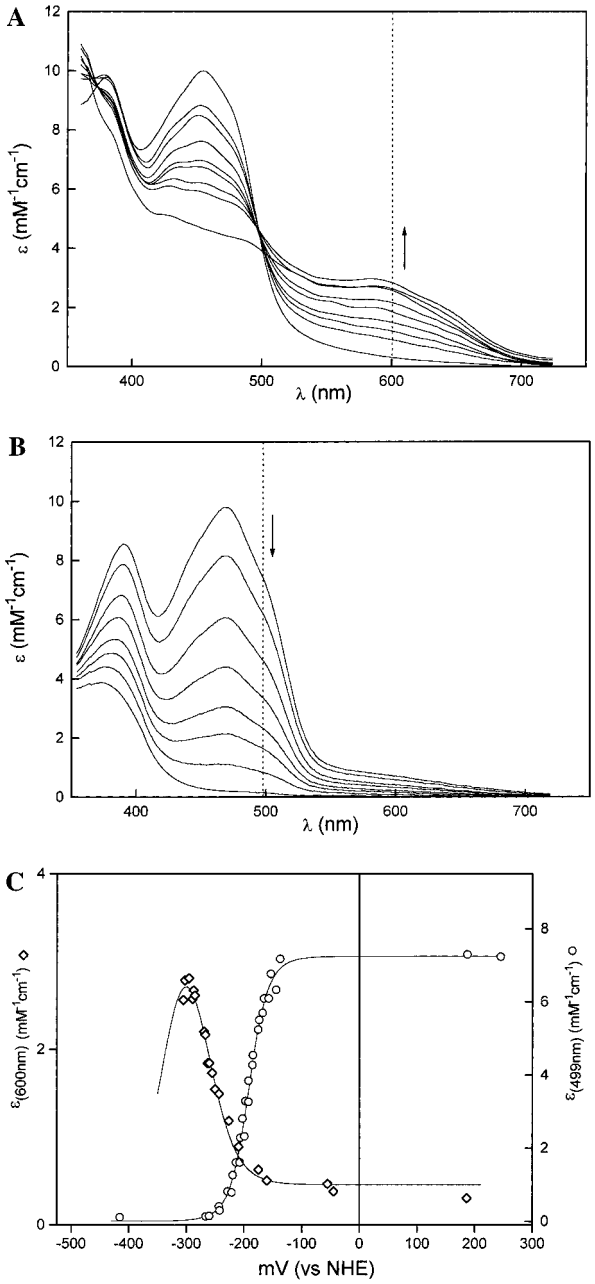

FIGURE 3: (A) Redox titration of the FAD domain conducted in 0.1 M phosphate buffer (pH 7.0) at 25 ± 2 °C. The direction of the arrow indicates absorbance increases at 600 nm observed during the course of the reductive titration. (B) Redox titration of the FMN domain conducted in 0.1 M phosphate buffer (pH 7.0) at 25 ± 2 °C. The direction of the arrow indicates absorbance decreases at 500 nm observed during the reductive titration. (C) Plot of extinction coefficient versus electrode potential at 499 nm (right *y*-axis, FMN domain) and 600 nm (left *y*-axis, FAD domain) fitted to eq 1 as described in the Results. From the 499 nm data, E'_1 (FMN) = −206 ± 13 mV and E'_2 (FMN) = −177 ± 12 mV; from the 600 nm data E'_1 (FAD) = −269 ± 10 mV and E'_2 (FAD) = −337 ± 19 mV.

oxidized/reduced couple is some 170 mV more negative than that of the FMN, it is unlikely that absorbance changes due to the heme will interfere with the analysis. However, the heme undergoes significant spectral changes at 600 nm and these would therefore complicate the analysis of the FAD reduction at this wavelength. For this reason, data recorded at 567 nm were used. At this wavelength, the interference from the heme is at its minimum. These data, primarily representing the reduction of FAD to semiquinone, were

Table 1: Midpoint Reduction Potentials [E' (mV)] for the Flavin and Heme Cofactors in P-450 BM3 and Its Constituent Domains, Calculated from Electrode Potential *vs* Absorbance Data as Described in the Results and in Figures 1−4[a]

	E'_{12}	E'_1	E'_2
diflavin FAD	−332 ± 4	−292 ± 4	−372 ± 4
diflavin FMN	−203 ± 6	−213 ± 5	−193 ± 6
holoenzyme FAD		−289 ± 4	
holoenzyme FMN	−196 ± 5	−216 ± 11	−177 ± 11
FAD domain	−303 ± 15	−269 ± 10	−337 ± 19
FMN domain	−192 ± 13	−206 ± 13	−177 ± 12
heme domain		−368 ± 6	
heme domain + palm		−265 ± 7	
heme domain + arac		−239 ± 6	

[a] All values were derived under the conditions of 100 mM phosphate buffer, pH 7.0, at a temperature of 25 ± 2 °C. E_{12} refers to $F_{ox} + 2e^- \leftrightarrow F_{red}$; E_1 refers to $F_{ox} + e^- \leftrightarrow F_{sq}$ or $H_{ox} + e^- \leftrightarrow H_{red}$; E_2 refers to $F_{sq} + e^- \leftrightarrow F_{red}$. (F ≡ flavin, H ≡ heme, e^- ≡ electron, ox ≡ oxidized, sq ≡ semiquinone, red ≡ reduced, palm ≡ palmitate, arac ≡ arachidonate).

fitted to a single-electron function. Reliable data beyond a value of −320 mV could not be obtained due to instability of the potential measured. This may reflect the reaction of dithionite breakdown products with the holoenzyme. This phenomenon is currently under further investigation. Therefore, it was not possible to estimate accurately the reduction potential of the holoenzyme FAD semiqinone/reduced couple. However, an estimate could be obtained for the FAD oxidized/semiquinone couple, which is the same, within error, as the value obtained for the diflavin domain. Both reduction potentials were obtained for the FMN from the data collected at 499 nm. These are also essentially the same as the values for the diflavin domain. In both data sets plotted in Figure 2B, fit ranges were chosen to minimize the influence of the other redox centers. That is, it is clear that in the 499 nm data that a small absorbance increase due to partial reduction of the heme occurs at potentials lower than −270 mV. This is excluded from the fitting process. Similarly, a small absorbance decrease is observed in the 567 nm data at potentials above −200 mV due to reduction of the FMN. This is also observed in the diflavin domain (see Figure 1B), where it has been compensated for in the fitting process.

FAD Domain and FMN Domain. Figure 3 (panels A and B) shows the redox titration of the FAD and FMN domains of P-450 BM3, monitored by UV−vis spectrophotometry between 350 and 800 nm. Figure 3C plots the values for the absorbance at 499 and 600 nm against the potential of the enzyme solution. These values were chosen to be consistent with the data presented for the diflavin domain and holoenzyme; although, in these single-cofactor domains there are none of the complicating factors described for the multidomain enzymes. Both data sets were fitted as two electron redox processes utilizing eq 1. The values for the FMN domain are consistent with this being the higher potential flavin and appear to be perturbed little by the separation of this domain from the FAD and heme domains, i.e., the two-electron process is only 11 mV higher than in the diflavin domain. Analysis of the data for the FAD domain was complicated by the propensity of the enzyme to form precipitate over the course of the experiment, especially at low potentials. For this reason, the quality of these data is less good. However, it is clear that the FAD is the low-potential flavin identified in the diflavin domain, with a stabilized blue semiquinone.

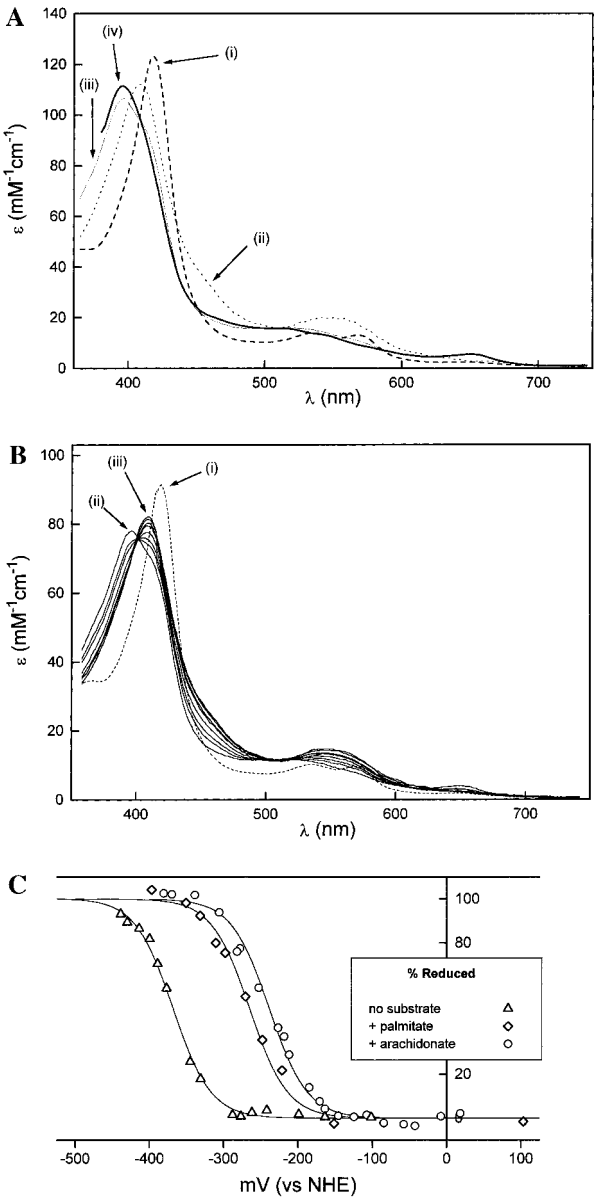

FIGURE 4: (A) Spectra of the P-450 BM3 heme domain (i) oxidized (dashed line), (ii) reduced (dotted line), (iii) oxidized + palmitate (thin solid line), (iv) + arachidonate (thick solid line). (B) Redox titration of P-450 BM3 heme domain in the presence of palmitate conducted in 0.1 M phosphate buffer (pH 7.0) at 25 ± 2 °C. Trace i is the oxidized palmitate-free heme domain and trace ii is the oxidized palmitate-bound heme domain. In subsequent traces, progressive reduction of the palmitate-bound heme domain by titration with sodium dithionite results in the formation of the fully reduced heme domain (iii) with absorbance maximum at 407 nm. (C) Plot of percentage reduced heme versus electrode potential for the substrate-free (no substrate) palmitate-saturated (+palmitate) and arachidonate-saturated (+arachidonate) forms of the heme domain, fitted to single electron redox functions with values for E' of −368 ± 6, −265 ± 7, and −239 ± 6 mV, respectively.

Hemes. Figure 4A shows the spectra of four different heme states: oxidized, reduced, oxidized/saturated with arachidonate, and oxidized/saturated with palmitate. The redox titrations described here represent the conversion of each of the three oxidized states into the universal reduced state. Figure 4B illustrates one of these titrations (oxidized/saturated with palmitate to reduced). Figure 4C plots the percentage reduced heme, calculated by integrating difference spectra of the reduced/oxidized samples between appropriate wavelengths, against electrode potential. All data were fitted to simple one-electron Nernst equations, parameters from which are contained within Table 1. In the absence of fatty acid substrate, the heme has a very negative potential (−370 mV) which is significantly lower than that of the initial electron source NADPH (−320 mV) and therefore essentially out of reach. Addition of substrate to the heme results in a shift in redox potential greater than +100 mV, bringing it well within range. However, it is also apparent that the shift induced by arachidonate is larger than that due to palmitate (129 *vs* 103 mV). This seems to correlate with the larger spectral change induced by arachidonate, indicating that a greater proportion of heme is pushed into the high-spin form (see Figure 4A).

DISCUSSION

This is the first manuscript in which the reduction potentials for all redox couples of an entire class II (E class) cytochrome P-450 system have been determined. The data presented indicate that control of fatty acid oxidation and prevention of futile cycling of electrons from NADPH is exerted at the level of binding of the fatty acid substrate, such that dehydration of the active site and conversion of the heme iron from a low-spin to a high-spin form is accompanied by a large increase in redox potential [possibly > 130 mV for a substrate-saturated active site, since even arachidonate (129 mV increase) may not induce a 100% spin-state shift]. This permits electron flow to occur to the heme iron and for subsequent steps including oxygen association and second electron transfer to the much higher potential ferrous−oxy intermediate to be completed rapidly while the substrate is enclosed in the active site. It is interesting to note that both NMR and X-ray crystal structure data are in agreement and indicate that substrate association is initially at too great a distance from the heme iron for oxidation, but that reduction of the heme iron facilitates structural change and the movement of substrate proximal to the heme (Modi *et al*., 1996; Li & Poulos, 1997).

The measured reduction potentials for the FAD and FMN coenzymes in all states are very similar for the holoenzyme, diflavin domain, and individual FAD and FMN domains. These data indicate that little perturbation in the environments of the flavins occur as genetic scission is used to express constructs of single and double domains of flavocytochrome P-450 BM3, which appears to be comprised of three major polypeptide domains. The forthcoming atomic structure of a eukaryotic cytochrome P-450 reductase indicates that the FAD and FMN in this enzyme are in close proximity and that direct electron transfer between the two (as opposed to a proteinaceous electron transfer pathway) is most probable (Kim *et al*., 1996). Given the apparent lack of effect on redox couples in the distinct FAD and FMN domains compared with BM3 diflavin domains, it might be the case that the two flavins are more spatially separated in the BM3 reductase than is the case for the eukaryotic forms. The fact that the spliced domains retain very similar redox factor characteristics is further evidence that P-450 BM3 has been formed from the fusion of at least three genes encoding a hemoprotein P-450 (heme domain), an NADPH-binding reductase (FAD domain), and a flavodoxin-like protein (FMN domain) (Porter, 1991). These data identify the high- and low-potential flavins of P-450 BM3 as the FMN and FAD, respectively. This is the same situation as for the mammalian liver P-450 reductase (Iyanagi et al., 1974). Indeed, at −332

mV (FAD) and −203 mV (FMN), the midpoint potentials for the two-electron reduction processes of the diflavin domain are very similar to those values reported for the mammalian reductase (−328 and −190 mV, respectively). However, while the midpoint potentials for the two single-electron flavin reduction processes are similar for the FADs of the BM3 reductase domain and the mammalian reductase ($E_1' = -292$ and −290 mV, and $E_2' = -372$ mV and −365 mV, respectively), the two single-electron potentials are much closer for the FMN in the BM3 reductase than for the mammalian form [$E_1' = -213$ and −110 mV, and $E_2' = -193$ and −270 mV, respectively (Iyanagi *et al*., 1974)].

Recently, quantitation by EPR of the blue flavin semiquinone signal observed on reduction of substrate-free P-450 BM3 holoenzyme or diflavin domain by NADPH showed there to be a single flavin semiquinone per molecule in NADPH-reduced BM3 holoenzyme and reductase domain, indicating that the NADPH is capable of reducing the diflavin domain of the enzyme only as far as the three electron form (Munro *et al*., 1996). The positive reduction potential difference in the semiquinone/hydroquinone couple for the FMN domain indicates that the hydroquinone form of this coenzyme is more thermodynamically favorable than is the semiquinone, in agreement with recent results from kinetic and titration studies (Govindaraj & Poulos, 1997; Sevrioukova *et al*., 1996). By contrast, the midpoint reduction potential of the diflavin domain FAD semiquinone/hydroquinone couple is considerably more negative than that of both the FAD oxidized/semiquinone couple and of NADPH itself. Clearly, the blue semiquinone observed resides on the FAD of P-450 BM3. These data are slightly surprising in view of the facts that the FMN domain is a flavodoxin-like polypeptide (Porter, 1991) and that the flavodoxins normally stabilize a (neutral) blue semiquinone form of their FMN. In P-450 BM3, it is the FAD and not the FMN which forms the blue semiquinone. Indeed, recent studies in this laboratory with *E. coli* flavodoxin and flavodoxin reductase [which have been reported previously to mimic the activity of eukaryotic P-450 reductase by supporting the activity of mammalian P-450s (Jenkins & Waterman, 1994)] indicate that it is the flavodoxin of this pair which stabilizes a blue semiquinone species (unpublished data).

Anaerobic reductive titrations of substrate-bound and substrate-free forms of the heme domain of P-450 BM3 yield spectra that are distinctly different from both those of the substrate-bound and substrate-free oxidized forms of the enzyme and from that of the aerobically dithionite-reduced substrate-free form. The absorbance maxima of the Soret band in these anaerobically reduced species are located at approximately 407 nm. Aerobic reductions of substrate-free heme domain generally result in a spectrum in which the Soret band is little moved from its position at around 419 nm, perhaps decreasing a little in intensity. Clearly, full reduction of the substrate-free heme is not achieved aerobically, likely due to rapid reduction of oxygen and/or sulfite (generated from dithionite) by the Fe^{2+} heme. The heme will thus return rapidly to the Fe^{3+} form, and an equilibrium will be formed in which the majority of heme at any time is in the oxidized form. On bubbling of carbon monoxide into dithionite-treated heme domain, however, the P-450 product is soon formed, since this equilibrium is pulled over to the reduced form by continual extraction of the Fe^{2+} heme present into the deadend CO−Fe^{2+} P-450 complex.

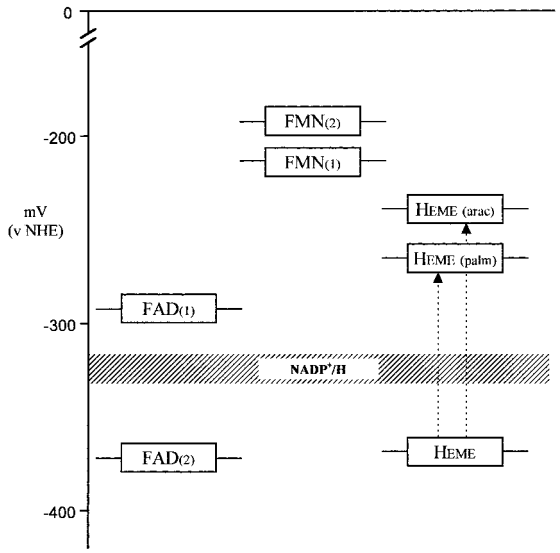

FIGURE 5: Comparison of the individual reduction potentials for FMN, FAD (both from the diflavin domain), and the heme of the heme domain both before and after saturation with palmitate (palm) and arachidonate (arac).

It is notable that certain fatty acid substrates of P-450 BM3 give markedly higher k_{cat} values than do others, e.g., arachidonate is oxidized at approximately 3−4 times the rate that laurate is. The order of increasing magnitudes of k_{cat} values for the different substrates of P-450 BM3 is broadly in line with the decreasing order of their K_m values. A logical extension of these data would be that catalytic rate for P-450 BM3 would be related to the ability of the different substrates to either saturate the active site of the protein or induce high levels of the low-spin to high-spin transition, with the latter explanation perhaps being the more likely. Clearly, many substrates (e.g., laurate) do not induce full spin-state conversions at saturating levels. As can be seen in Figure 4A (iv), the absorbance of the near-fully-high-spin heme (arachidonate-induced) is one in which the Soret band at approximately 390 nm is of very similar magnitude to that of the the oxidized substrate-free band at 419 nm. Previously reported spectra for fatty acid-bound heme domain of P-450 BM3 [e.g., lauric acid (Modi *et al*., 1995)] show only partial high-spin heme conversion. The use of transient kinetics to study the effect of different substrates on the microscopic rate constants of P-450 BM3 indicates that electron transfers through the flavins are unaltered, but that rates of electron transfer to the heme iron (as measured by the rate of formation of the ferrous−carbon monoxide adduct at 450 nm) are markedly affected by different substrates (e.g., first-order rate constants for laurate of approx. 130 s^{-1} and myristate of approx. 220 s^{-1}) (Munro *et al*., 1996). Clearly, ability of substrates to convert P-450 BM3 heme to the high-spin form is key to catalytic efficiency.

The data presented here clearly demonstrate the electron transfer pathway through the coenzymes of flavocytochrome P-450 BM3 (Figure 6). Hydride transfer from NADPH is the first step in the electron transfer pathway and results in the transient formation of an FAD hydroquinone. This species is thermodynamically unfavorable and transfers electrons to the much higher potential FMN, the hydroquinone of which is thermodynamically favored over the semiquinone. Electron transfer from FMN hydroquinone to the heme cannot occur in the absence of fatty acid substrate.

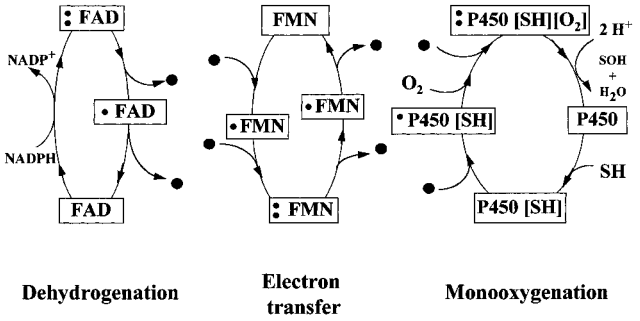

FIGURE 6: A schematic representation of the catalytic cycle of P-450 BM3. Electrons are represented as black circles. Hydride transfer from NADPH results in transient formation of FAD hydroquinone. This is unstable and, since the potential of both FMN semiquinone and hydroquinone are more positive than those of their FAD counterparts, electrons are transferred to the FMN. Electron transfer from FMN to heme cannot occur until substrate (SH) is bound. Thereafter, one electron is transferred to form ferrous heme, which binds dioxygen. A second electron is passed to this high-potential species, and rapid oxygenation of substrate ensues. Dissociation of oxygenated substrate (SOH) regenerates the oxidized resting-state P-450.

Under aerobic conditions, substrate-free P-450 BM3 catalyzes electron transfer to oxygen at rates of around 2 min^{-1}. The constituent diflavin domain catalyzes the process with a similar rate, indicating that this low rate of electron leak is mediated by the flavin coenzymes (Munro *et al.*, 1995). Gating of electron transfer to the catalytic center occurs by a fatty acid substrate-modulated increase in heme reduction potential, elevating the midpoint potential of the heme to a point at which electron transfer from the FMN becomes feasible. It should be remembered that, although the heme midpoint reduction potential value measured in the presence of a good substrate (arachidonate) is only of similar magnitude (slightly lower), to that of the FMN semiquinone and hydroquinone, this value represents an "average" potential for all low-spin and high-spin molecules in the mixture. As discussed above, even arachidonate does not convert the enzyme to a completely high-spin state, although an increase in midpoint reduction potential of 129 mV was observed for a saturated solution of the fatty acid. The midpoint reduction potential for a 100% high-spin heme population is likely to be slightly higher than that measured and possibly above those of the FMN semiquinone and hydroquinone. Notwithstanding this, it is obvious that the midpoint reduction values for FMN and high-spin heme are sufficiently similar that rapid equilibration of electrons will occur and that a significant proportion of the heme will be reduced by the FMN in substrate-bound P-450 BM3. On single-electron reduction, the ferrous heme iron will bind oxygen and this high-potential intermediate will be further reduced rapidly with a second electron from FMN. Thus, the first electron transfer can be considered as initiating an essentially irreversible chain of events which lead to substrate monooxygenation (Figure 6). In the presence of good substrates, tightly coupled oxidation of fatty acid occurs with rates usually well in excess of 1000 min^{-1}. Indeed, for palmitate a rate of 4600 min^{-1} has been reported (Narhi & Fulo, 1986).

It is well-known that preincubation of fatty acid-free P-450 BM3 with NADPH leads to time-dependent decreases in the hydroxylase activity of the enzyme (Narhi & Fulco, 1986). It is possible that a time-dependent conformational change occurs on prolonged incubation with NADPH such that electron transfer to the heme domain is diminished. Moreover, addition of fatty acid (laurate) to P-450 BM3 stimulates cytochrome *c* reduction through the diflavin domain, and enhanced flavin fluorescence has been reported on fatty acid binding to P-450 BM3 (Murataliev & Feyereisen, 1996). These data suggest that fatty acid binding may induce conformational alteration in the diflavin domain of P-450 BM3, a process possibly involved in regulation of catalysis. Another possible regulatory mechanism may be via modulation of flavin reduction potential(s) by bound NADP(H), as suggested recently by Murataliev *et al*. (1997). It is possible that, subsequent to hydride transfer from NADPH to the FAD of P-450 BM3, the bound $NADP^+$ stabilizes a two-electron-reduced species with both FAD and FMN in the semiquinone state, through ionic interaction of $NADP^+$ with an FAD anionic semiquinone. These authors postulate that this situation is achieved through the elevation of the midpoint potential of FAD when $NADP^+$ is bound; a similar situation to that observed previously with the FAD proteins adrenodoxin reductase (Lambeth & Kamin, 1976) and cytochrome *b*5 reductase (Iyanagi, 1977). Such a phenomenon may explain how P-450 BM3 avoids the accumulation of an inactive three-electron-reduced form on reaction with NADPH. The relatively slow buildup of this inactivated form may occur only after dissociation of $NADP^+$ and the binding and electron transfer from a second molecule of NADPH (Murataliev *et al*., 1997; Munro *et al*., 1996). The possibility that $NADP^+$ binding may modulate flavin potentials in P-450 BM3 is under investigation in this laboratory. Clearly, the electron transfer through P-450 BM3 is elegantly controlled by the redox properties of its coenzymes. Conformational as well as redox control mechanisms may also prove important.

In this manuscript, we have used redox potentiometry to identify clearly the pathway of electron transfer though P-450 BM3. The data obtained not only confirm that a substrate-dependent reduction potential increase underlies control of the fatty acid oxidation, but also provide evidence for the discrete multidomain structure of the enzyme. In addition, we now have important references for the comparison of the redox properties of mutant enzymes. This will be of particular importance in the analysis of active site alterations, such as the spin-state perturbations caused by mutagenesis at residue W96 (Munro *et al*., 1994). Our current studies are directed towards characterisation of such mutants.

REFERENCES

Dutton, P. L. (1978) *Methods Enzymol. 54*, 411−435.

Govindaraj, S., & Poulos, T. L. (1997) *J. Biol. Chem. 272*, 7915−7921.

Guengerich, F. P. (1988) *Cancer Res. 48*, 2946−2954.

Iyanagi, T. (1977) *Biochemistry 16*, 2725−2730.

Iyanagi, T., Makino, N., & Mason, H. S. (1974) *Biochemistry 13*, 1701−1710.

Jenkins, C. M., & Waterman, M. R. (1993) *J. Biol. Chem. 269*, 27401−27408.

Kim, J. J. P., Roberts, D. L., Djordevic, S., Wang, M., Shea, T. M., & Masters, B. S. S. (1996) *Methods Enzymol. 272*, 368−377.

Lambeth, J. D., & Kamin, H. (1976) *J. Biol. Chem. 251*, 4299−4306.

Li, H.-Y., & Poulos, T. L. (1997) *Nat. Struct. Biol. 4*, 140−146.

Martinis, S. A., Blanke, S. R., Hager, L. P., & Sligar, S. G. (1996) *Biochemistry 35*, 14530−14536.

Miles, J. S., Munro, A. W., Rospendowski, B. N., Smith, W. E., McKnight, J. & Thomson, A. J. (1992) *Biochem. J. 288*, 503−509.

Modi, S., Primrose, W. U., Boyle, J. M. B., Gibson, C. F., Lian, L.-Y., & Roberts, G. C. K. (1995) *Biochemistry 34*, 8982−8988.

Mueller, J., Loida, P. L., & Sligar, S. G. (1995) in *Cytochrome P450; Structure, Mechanism and Biochemistry*, 2nd ed. (Ortiz de Montellano, P. R. O., Ed.) pp 83−124, Plenum Press, New York.

Munro, A. W., & Lindsay, J. G. (1996) *Mol. Microbiol. 20*, 1115−1125.

Munro, A. W., Lindsay, J. G., Coggins, J. R., Kelly, S. M., & Price, N. C. (1994a) *FEBS Lett. 343*, 70−74.

Munro, A. W., Malarkey, K., Lindsay, J. G., Coggins, J. R., Price, N. C., Kelly, S. M., McKnight, J., Thomson, A. J., & Miles, J. S. (1994b) *Biochem. J. 303*, 423−428.

Munro, A. W., Lindsay, J. G., Coggins, J. R., Kelly, S. M., & Price, N. C. (1995) *Biochim. Biophys. Acta 1231*, 255−264.

Munro, A. W., Daff, S., Coggins, J. R., Lindsay, J. G., & Chapman, S. K. (1996) *Eur. J. Biochem. 239*, 403−409.

Murataliev, M. B., & Feyereisen, R. (1996) *Biochemistry 35*, 15029−15037.

Murataliev, M. B., Klein, M., Fulco, A. J., & Feyereisen, R. (1997) *Biochemistry 36*, 8401−8412.

Narhi, L. O., & Fulco, A. J. (1986) *J. Biol. Chem. 261*, 7160−7169.

Narhi, L. O., & Fulco A. J. (1987) *J. Biol. Chem. 73*, 1078−1082.

Porter, T. D. (1991) *Trends Biochem. Sci. 16*, 154−158.

Poulos, T. L., Finzel, B. C., & Howard, A. J. (1987) *J. Mol. Biol. 195*, 687−700.

Sevrioukova, I., Truan, G., & Peterson, J. A. (1996) *Biochemistry 35*, 7528−7535.

Sligar, S. G., & Gunsalus, I. C. (1976) *Proc. Natl. Acad. Sci. U.S.A. 73*, 1078−1082.

Wright, R. L., Harris, K., Solow, B., White, R. H., & Kennelly, P. J. (1996) *FEBS Lett. 384*, 235−239.

BI971085S